Construction of Convex Inner Approximations of Optimal Power Flow Feasibility Sets

Hung D. Nguyen, Krishnamurthy Dvijotham, and Konstantin Turitsyn

***Abstract*—The non-convexity of the ACOPF problem rooted in nonlinear power flow equality constraints poses harsh challenges in solving it. Relaxation techniques are widely used to provide an estimation of the optimal solution. In this paper, we propose a scalable optimization framework, on the other hand, for estimating convex inner approximations of the power flow feasibility sets based on Brouwer fixed point theorem. The self-mapping property of fixed point form of power flow equations is certified using the adaptive bounding of nonlinear and uncertain terms. The resulting nonlinear optimization problem is non-convex; however, every feasible solution defines a valid inner approximation and the number of variables scales linearly with the system size. The framework can naturally be applied to other nonlinear equations with affine dependence on inputs. Test cases up to 1354 buses are used to illustrate the scalability of the approach. The results show that the approximated regions are not conservative and cover large fractions of the true feasible domains.**

***Index Terms*—Feasibility, OPF, inner approximation, solvability, nonconvexity.**

I. Introduction

The AC optimal power flow (ACOPF) representation of power system forms a foundation for most of the normal and emergency decisions in power systems. Since it was first introduced in 1962, the OPF problem has been one of the most active research areas in power system community. Being an NP-hard problem, it still lacks a scalable and reliable optimization algorithm [1] although last years were marked by a tremendous progress in this area [2]–[5].

Relaxations of power flow equations provide a means for constructing outer approximations of the non-convex feasibility sets in voltage/phase domain via tractable convex envelopes. By the nature of outer approximations, convex relaxations can generally be used for establishing certificates of insolvability of power flow equations [6] and can be naturally used to for estimation of loadability margins.

At the same time, the reverse problem of establishing inner approximations of feasibility sets although appearing in many contexts is still open. Most naturally, inner approximations of feasibility sets in power injection space can be used to assess the robustness of a given operating point to uncertainties in renewable or load power fluctuations. They can also be used to enforce feasibility in situations where constraining the system to nonlinear power flow equations and operational specifications is not practical. For example, in real-time corrective emergency control where the computation time is critical or in complex high-level optimization that is too complex to incorporate nonlinear constraints. Similarly, the reduced size inner approximations can be enforced in situations where instead of the regular feasibility, an additional margin is required from the solutions concerning load/renewable uncertainty. Whenever the approximation has a special geometric structure, it can also be naturally used for the design of decentralized decision making, for example, allowing for independent and communication-free redispatch of power resources in different buses/areas.

Like many other power system problems, the original setting for construction of inner approximations of power flow feasibility sets was introduced by Schweppe and collaborators in late 70s [7]. The first practical algorithms based on fixed point iteration appeared in early 80s [8]. In the Soviet Union, the parallel effort focused on the problem of constructing solvability sets for static swing equations [9], [10]. More recently, new algorithms based on different fixed point iterations have been proposed for radial distribution grids without PV buses [11]–[14], decoupled power flow models equivalent to resistive networks with constant power flows [15] and lossless power systems [16], [17]. Although more general approaches that do not rely on special modeling assumptions have been proposed in the literature [18]–[20], they still suffer from either poor scalability or high conservativeness or both.

In this work, we develop sufficient conditions for the existence of feasible power flow solutions, based on which we propose a novel algorithmic approach to constructing inner approximations of OPF feasibility domains that can apply to the most general formulation of power flow equations without any restrictions on the network and bus types. The size of the resulting regions is comparable to the actual feasibility domain even for large-scale models and can be potentially improved in the future. In comparison to most of the other approaches cited above, the inner approximations developed in this work are not given by a closed-form expression but instead are constructed by solving an auxiliary optimization problem defined in (19). This optimization problem, although being non-convex, allows for fast construction of the inner approximations. Any feasible solution to this problem, even a suboptimal one establishes a region where the solution of the original power flow is guaranteed to exist and satisfy feasibility constraints. Performance of the proposed algorithm is validated on several medium and large sized IEEE test cases.

The structure of the rest of the paper is the following. After introducing the general ACOPF feasibility problem in II, we continue to formulate the central optimization problem

Hung D. Nguyen and Konstantin Turitsyn are with the Department of Mechanical Engineering, Massachusetts Institute of Technology, Cambridge, MA, 02139 USA e-mail: hunghtd@mit.edu, and turitsyn@mit.edu. Krishnamurthy Dvijotham is with Google Deepmind, London, UK. e-mail:dvij@cs.washington.edu

in section III applicable to any nonlinear system with affine inputs. The general technique is adapted to power flows in section IV and is validated numerically in section V.

II. Notation and an OPF formulation

We start off this section by introducing the set of notation which will be used in this paper. We use $\mathbb{C}$ to denote the set of complex number. $\overline{\boldsymbol{x}}$ denotes the conjugate of $\boldsymbol{x} \in \mathbb{C}^n$. The Jacobian of a set of functions is defined as $(\frac{\partial f}{\partial x})_{ij} = \frac{\partial f_i}{\partial x_j}$ for $f : \mathbb{C}^n \mapsto \mathbb{C}^n$. The considered system has the graph $\mathcal{V}$ and the load and generator sets denoted by $\mathcal{L}$ and $\mathcal{G}$, respectively. Further, $\mathcal{E}$ is a set of unordered lines $e = (k,l) = (l,k)$, $k,l \in \mathcal{V}$. The $\odot$ operator stands for element-wise product $[x \odot y]_i = x_i y_i$ for $x, y \in \mathbb{R}^n$.

In this work, we study a general ACOPF subject to:

$$p_k + jq_k = \sum_l V_k \overline{Y}_{kl} V_l \exp(-j\theta_e), \quad k \in (\mathcal{L}, \mathcal{G}) \tag{1}$$

$$V_k^{min} \leq V_k \leq V_k^{max}, \quad k \in \mathcal{L} \tag{2}$$

$$\theta_e^{min} \leq \theta_e \leq \theta_e^{max}, \quad e \in \mathcal{E} \tag{3}$$

$$p_k^{min} \leq p_k \leq p_k^{max}, \quad k \in \mathcal{G} \tag{4}$$

$$q_k^{min} \leq q_k \leq q_k^{max}, \quad k \in \mathcal{G} \tag{5}$$

$$|s_e^f| \leq s_e^{max}, \quad |s_e^t| \leq s_e^{max}, \quad e \in \mathcal{E}. \tag{6}$$

Each bus $k \in \mathcal{V}$ of the system is characterized by a complex voltage $v_k = V_k \exp(\theta_k)$ and apparent power generation/consumption $s_k = p_k + jq_k$. For each edge or line e connecting bus k and bus l, we define an angle difference $\theta_e = \theta_k - \theta_l$. The apparent power transfer s_e through the line e can be either "from" or "to" flow which is denoted by the superscripts f and t.

More compactly, we use the notation u to denote the vector of parameters, i.e. $u = [p_{\mathcal{G}}; p_{\mathcal{L}}; q_{\mathcal{L}}; V_{\mathcal{G}}]$ and use x to denote the space of variables, i.e. $x = [\theta_{\mathcal{G}}; \theta_{\mathcal{L}}; V_{\mathcal{L}}; q_{\mathcal{G}}]$. In the following, we formally define the main focus of the paper, the feasible set of the OPF problem. The feasible set of the OPF problem is the set of control inputs, u, with which the power flow equations (1) has at least one feasible solution which satisfies all concerned operational constraints (2) to (6).

OPF feasible set is often non-convex and even not single connected. The OPF problem belongs to the class of non-convex optimization problem which are challenging and inefficient to solve. In this work, we construct convex inner approximations of this set of polytopic form. Mathematically, they represent sufficient conditions of existence of feasible solution that can be quickly checked or enforced in applications where optimality of the power flow solution is not critical.

III. The feasibility of input-affine systems

In this section, we develop our general approach for deriving sufficient conditions for the existence of a feasible solution to a nonlinear constrained system. Our approach applies to a broad class of nonlinear systems that satisfy two essential properties: they depend affinely on the input variables, and their nonlinearity can be expressed regarding a linear combination of nonlinear terms that admit simple bounds.

Consider a following set of nonlinear equations on $x \in \mathbb{R}^n$ that depend in affine way on the vector of inputs $u \in \mathbb{R}^k$ represented:

$$Mf(x) - Ru = 0 \tag{7}$$

where the solution is subject to two classes of constraints:

$$x^{min} \leq x \leq x^{max} \tag{8}$$

$$h(x) \leq 0 \tag{9}$$

Here $M \in \mathbb{R}^{n \times m}$, $R \in \mathbb{R}^{n \times k}$, and $f = [f_1; f_2; \ldots; f_m] : \mathbb{R}^n \to \mathbb{R}^m$ is the set of nonlinear "primitives", i.e. simple nonlinear terms usually depending on few variables. Without any loss of generality, we assume that $h(x) : \mathbb{R}^n \to \mathbb{R}^l$ can be expressed in terms of the same nonlinear primitives function $f(x)$, i.e., $h(x) = Tf(x)$ with $T \in \mathbb{R}^{l \times m}$.

Next, assume also that there exists a *base solution* $u^\star \in \mathbb{R}^k, x^\star \in \mathbb{R}^n$ such that $Ru^\star = Mf(x^\star)$. Furthermore, let

$$J(x) = M \left.\frac{\partial f}{\partial x}\right|_x, \; [J(x)]_{ij} = \sum_{k=1}^m M_{ik} \frac{\partial f_k}{\partial x_j}, \tag{10}$$

denote the Jacobian of the system of equations, while $J_\star = J(x^\star)$ be the Jacobian evaluated at the base solution that we assume to be non-singular. In power system context, the normal operating point is a typical base solution.

In the following paragraphs, we will derive a fixed-point point representation of system (1) that allows for simple certification of solution existence. This solvability certificate is based on the bounds on nonlinearity in the neighborhood of the base operating point. Compact representation of the corresponding convex regions in the input, state and nonlinear image spaces will be introduced below to facilitate our development.

For any differentiable nonlinear map $f : \mathbb{R}^n \to \mathbb{R}^m$ and a base point $x^\star \in \mathbb{R}^n$ we define a nonlinear "residual" map $\delta f(x)$ and $\delta_2 f(x)$ as the following combinations of $f(x)$, base value $f^\star = f(x^\star)$ and base Jacobian $\partial f / \partial x|_{x^\star}$:

$$\delta f(x) = f(x) - f^\star \tag{11}$$

$$\delta_2 f(x) = f(x) - f^\star - \left.\frac{\partial f}{\partial x}\right|_{x = x^\star} \cdot (x - x^\star) \tag{12}$$

The defined residual operator allows for compact representation of the original system (3) in the fixed-point form:

$$x = x^\star + J_\star^{-1} R(u - u^\star) - J_\star^{-1} M \delta_2 f(x). \tag{13}$$

or, even more compactly as

$$\tilde{x} = F(\tilde{x}; \tilde{u}) = J_\star^{-1} R \tilde{u} + \phi(\tilde{x}), \tag{14}$$

where $\tilde{x} = x - x^\star$ and $\tilde{u} = u - u^\star$ denote the deviations of the variable and input vector from the base solution and $\phi(\tilde{x}) = -J_\star^{-1} M \delta_2 f(x^\star + \tilde{x})$ represents the nonlinear corrections. It is important to note that the Jacobian J is not $\partial f / \partial x$, but the one defined in (10).

Next, we assume that the input deviations $\tilde{u}$ belong to a structured box-shaped uncertainty set $\mathcal{U}$ defined as $-\ell_u^- \leq \tilde{u} \leq \ell_u^+$ or more compactly as $\mathcal{U}(\ell_u) = \left\{\tilde{u} \in \mathbb{R}^L | \pm \tilde{u} \leq \ell_u^\pm \right\}$. Also, we use ℓ_u to denote $\ell_u = [\ell_u^-; \ell_u^+]$.

Having the fixed point form (14), we will apply the Brouwer's fixed point theorem (Chapter 4, Corollary 8 in [21]) stated below to derive a sufficient condition for solvability.

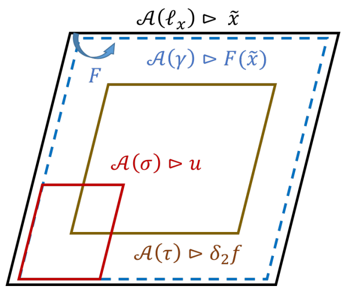

Fig. 1. Self-mapping function for a fixed-point form

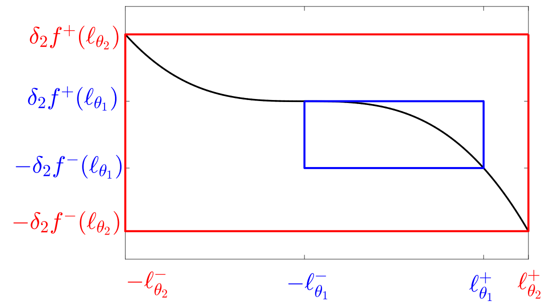

Fig. 2. Nonlinear bounds for $\delta_2\{\sin(\theta)\} = \sin(\theta) - \theta$ for two values of ℓ_θ: $\ell_{\theta_1} = [0, 0.4]$ and $\ell_{\theta_2} = [0.4, 0.5]$

Theorem 1 (Brouwer's fixed point theorem)**.** *Let $F : \mathcal{X} \mapsto \mathcal{X}$ be a continuous map where $\mathcal{X}$ is a compact and convex set in $\mathbb{R}^n$. Then the map has a fixed point in $\mathcal{X}$, namely $F(x) = x$ has a solution in $\mathcal{X}$.*

In this work we propose to use a parameterized polytope representation of $\mathcal{X} = \mathcal{A}(\ell_x)$ with a fixed face orientation but varying distances to individual faces. We refer to this set as an "admissibility polytope".

Formally, the admissibility polytope family $\mathcal{A}(\ell_x)$ defines the following non-empty polytope for any non-zero matrix of bounds $\ell_x = [-\ell_x^-, \ell_x^+] \in \mathbb{R}_+^{k\times 2}$:

$$\mathcal{A}(\ell_x) = \{\tilde{x} \in \mathbb{R}^n | \pm A\tilde{x} \le \ell_x^\pm\} \tag{15}$$

where $\pm A\tilde{x} \le \ell_x^\pm$ is shorthand for the following:

$$\{A\tilde{x} \le \ell_x^+, -A\tilde{x} \le \ell_x^-\} \equiv -\ell_x^- \le A\tilde{x} \le \ell_x^+$$

The polytope $\mathcal{A}(\ell_x)$ will be used to establish the neighborhoods of the base operating point where the solution is guaranteed to exist. Extra conditions of the form $\ell_x \le \ell_x^{\max}$ can be then used to impose additional "feasibility" constraints on the solution, such as voltage and line angle difference bounds. To prove the existence of the solution, we need to show the self-mapping of this polytope under the nonlinear map $F(\tilde{x}; \tilde{u})$. The most critical step in certifying the self-mapping is the establishment of nonlinearity bounds. Specifically, we assume that whenever the system is inside the admissibility polytope, i.e., $\tilde{x} \in \mathcal{A}(\ell_x)$, the nonlinear residual terms $\delta_2 f \in \mathbb{R}^m$ can also be naturally bounded explicitly based on ℓ_x. These bounds are formalized via "bounding polytope family" defined as follows. The nonlinear bounding polytope family $\mathcal{N}(\ell_x)$ certifies the following bounds on the nonlinear map $f : \mathbb{R}^n \to \mathbb{R}^m$:

$$\tilde{x} \in \mathcal{A}(\ell_x) \Longrightarrow \delta_2 f(x^\star + \tilde{x}) \in \mathcal{N}(\ell_x) \tag{16}$$

In other words, the nonlinear bounding polytope family establishes a bound on the nonlinear function given the bounds on its argument. In this work, we rely on the simple, though not particularly tight bounds illustrated on Figure 2 and formally represented by the functions $\delta_2 f_k^\pm(\ell_x)$

$$\mathcal{N}(\ell_x) = \{z \in \mathbb{R}^m | \pm z_k \le \delta_2 f_k^\pm(\ell_x)\} \tag{17}$$

Given the definition of the three convex polytopes $\mathcal{U}(\ell_u), \mathcal{A}(\ell_x), \mathcal{N}(\ell_x)$ we can restate the Brouwer fixed point theorem in the following form:

Corollary 1. *(Self-mapping condition) Suppose there exist bounds ℓ_x, ℓ_u such that*

$$\tilde{x} \in \mathcal{A}(\ell_x),\ \tilde{u} \in \mathcal{U}(\ell_u) \implies F(\tilde{x}; \tilde{u}) \in \mathcal{A}(\ell_x). \tag{18}$$

Then (14) *is solvable for all $\tilde{u} \in \mathcal{U}(\ell_u)$ and has at least one solution inside admissibility polytope: $\tilde{x} \in \mathcal{A}(\ell_x)$.*

We visualize the self-mapping condition in Figure 1. In Appendix A, we derive explicit condition on ℓ_x, ℓ_u that guarantee satisfaction of (18). The condition allows us to formulate the following optimization process which is a central result of this paper.

Construction of optimal inner approximation. Given the definitions introduced above, assume that the quality of the inner approximation is given by the cost function $c(\ell_x, \ell_u)$. Then the best approximation can be constructed by solving the following optimization problem:

$$\begin{aligned} &\max_{\ell_x, \ell_u} c(\ell_x, \ell_u) \quad \text{subject to :} \\ &\ell_x^\pm \ge B^+\ell_u^\pm + B^-\ell_u^\mp + C^+\delta_2 f^\pm(\ell_x) + C^-\delta_2 f^\mp(\ell_x) \\ &\ell_x \le \ell_x^{\max} \\ &D^+\ell_u^+ + D^-\ell_u^- + E^+\delta_2 f^+(\ell_x) + E^-\delta_2 f^-(\ell_x) + h_\star \le 0. \end{aligned} \tag{19}$$

Here $h_\star = h(x_\star)$ and the matrices B, C, D, E are given by $B = AJ_\star^{-1}R$, $C = -AJ_\star^{-1}M$, $D = TLJ_\star^{-1}R$, and $E = T - TLJ_\star^{-1}M$ and $L = \partial f/\partial x|_{x_\star}$. The upper indices $^\pm$ on the matrices refer to the absolute values of the positive and negative parts of these matrices, i.e., for any matrix F, $F = F^+ - F^-$ with $F_{ij}^\pm \ge 0$.

Problem (19) is non-convex and nonlinear program in the space of uncertainty and admissibility polytope shapes ℓ_u, ℓ_x. Although the optimal solution to this problem cannot be reliably found in polynomial time, any feasible solution to (19) establishes a certified inner approximation of the feasibility set. So, the natural strategy is to solve this problem is based on local optimization schemes. The local search is guaranteed to produce some feasible certificate because small enough values of ℓ_x are always feasible. This follows from the superlinear behavior of $\delta_2 f^\pm(\ell_x)$ in the neighborhood of $\ell_x = 0$.

The nonlinear program (19) can be further extended using linear relaxation, for example, the one presented in Appendix B-B. The advantages are twofold. First, it is much more cost-effective to solve the relaxed LP than to solve the original nonlinear problem. As shown in the simulation section V, we can construct the feasibility region efficiently for a large-scale power system of 1354 buses with the LP formulation. Second, the optimal solution obtained from the LP problem can be "fed" into the original nonlinear construction (19) as a non-trivial initialization. A local search scheme is then deployed to improve such an initial guess.

Further, the objective function $c(\ell_x, \ell_u)$ can be tailored to a specific use case of the resulting polytope. Below we present three possible choices for the certificate quality function $c(\ell_x, \ell_u)$ for common problems arising in power system analysis.

A. Natural certificate quality functions $c(\ell_x, \ell_u)$

1) Maximal feasible loadability set: A classical problem arising in many domains, including power systems, is to characterize the limits of system loadability characterized by a single stress direction in power space. In this case, the only column of the matrix R defines the stress direction, while the positive scalar u defines the feasible loadability level. The goal of the feasible loadability analysis is to find the maximal level u for which the solution still exists and is feasible. According to Corollary 3, all u satisfying $u^\star - \ell_u^- \leq u \leq u^\star + \ell_u^+$ are certified to have a solution, hence the objective function of (19) is simply $c(\ell_x, \ell_u) = \ell_u^+$. Of course, the simple loadability problem can be more easily solved using more traditional approaches like the continuation method.

2) Robustness certificate: In another important class of applications, the goal is to characterize the robustness of a given solution concerning some uncertain inputs. In power system context it could be the robustness concerning load or renewable fluctuations. Assume, without the loss of generality that the input variable representation is chosen in a way that all the components of $\tilde{u}$ are uniformly uncertain around with uncertainty set centered at zero. In this case the goal is to find the largest value of λ, such that the feasible solution exists for any $\tilde{u}$ satisfying $|\tilde{u}_k| \leq \lambda$ for all k. This problem can be naturally solved by maximizing $c(\ell_x, \ell_u) = \lambda$ with an extra set of uniformity constraints $[\ell_u^\pm]_k = \lambda$ ensuring that the box $\mathcal{U}$ represents a symmetric cube.

3) Chance certificates: In another popular setting one assumes some probability distribution of the uncertain inputs and aims to find a polytope that maximizes the chance of randomly sampled input being certified to have a solution. This problem can also be naturally represented in the generic certificate optimization framework. Assume, without major loss of generality that the inputs are i.i.d. normal variables. In this case, the log-probability $\mathbf{P}$ of a random sample falling inside the box $\mathcal{U}(\ell_u)$ is given by

$$\log \mathbf{P}(\ell_u) = \frac{1}{2}\sum_k \operatorname{erf}\left(\frac{[\ell_u^+]_k}{\sqrt{2}}\right) - \operatorname{erf}\left(-\frac{[\ell_u^-]_k}{\sqrt{2}}\right) \tag{20}$$

The maximal chance certificate is established by maximizing $c(\ell_x, \ell_u) = \log \mathbf{P}(\ell_u)$ within the central optimization problem.

IV. OPF FEASIBILITY

In this section, we apply the framework developed in previous sections to the power flow feasibility problem. There are many possible ways to represent the power flow equations in the form (7) amenable to the algorithm application. Moreover, the representation of the equation and the choice of nonlinear functions and their variables has a dramatic effect on the size of the resulting regions. We have experimented with a variety of formulations, most importantly traditional polar and rectangular forms of power flow equations with different choices of matrix M and function f in (7). In this manuscript, we present only one formulation that resulted in the least conservative regions for large-scale systems. This formulation is based on the admittance representation of the power flow equations and nonlinear terms associated with power lines. It can naturally deal with strong (high admittance) power lines in the system that are the main source of conservativeness for most of the formulations.

A. Admittance based representation of power flow

The power formulation discussed below is based on a non-traditional combination of node-based variables and branch-based nonlinear terms. This representation is naturally constructed using the weighted incidence type matrices. Specifically, we use $y^d \in \mathbb{C}^{|\mathcal{V}|}$ to represent the diagonal of the traditional admittance matrix, and matrices $Y^f, Y^t \in \mathbb{C}^{|\mathcal{V}|\times|\mathcal{E}|}$ as weighted incidence matrices representing the admittances of individual elements with Y^f corresponding to negative admittance of lines starting at a given bus, and Y^t corresponding to admittance of lines ending at it. Any power line with admittance y_e connecting the bus $\mathrm{from}(e)$ to the bus $\mathrm{to}(e)$ contributes to the two elements in the matrices Y^f and Y^t, specifically $Y^f_{\mathrm{from(e)},e} = -y_e$ and $Y^t_{\mathrm{to}(e),e} = y_e$. In this for a bus k consuming the complex current i_k, the Kirchoff Current Law takes the form

$$i_k = y_k^d v_k + \sum_e Y_{ke}^f v_{\mathrm{to}(e)} + Y_{ke}^t v_{\mathrm{from}(e)}. \tag{21}$$

Whenever the PQ bus is considered with constant complex power injection s_k, one also has $\overline{i_k} = s_k/v_k$. Next, we introduce the logarithmic voltage variables as $\rho_k = \log(V_k)$ and $\rho_e = \rho_{\mathrm{from}(e)} - \rho_{\mathrm{to}(e)}$ and rewrite the power flow equations in the following form:

$$y_{\mathcal{V}} - y_{\mathcal{V}}^d = Y_{\mathcal{V}\mathcal{E}}^t \mathrm{e}^{\rho_{\mathcal{E}} + j\theta_{\mathcal{E}}} + Y_{\mathcal{V}\mathcal{E}}^f \mathrm{e}^{-\rho_{\mathcal{E}} - j\theta_{\mathcal{E}}} \tag{22}$$

where $y_k = \overline{s_k}/|v_k|^2$. Assuming that the base solution is given by $\rho^\star, \theta^\star$ the equations can be rewritten as

$$y_{\mathcal{V}} - y_{\mathcal{V}}^d = \hat{Y}_{\mathcal{V}\mathcal{E}}^t \mathrm{e}^{\delta\rho_{\mathcal{E}} + j\delta\theta_{\mathcal{E}}} + \hat{Y}_{\mathcal{V}\mathcal{E}}^f \mathrm{e}^{-\delta\rho_{\mathcal{E}} - j\delta\theta_{\mathcal{E}}} \tag{23}$$

with $\hat{Y}^t = Y^t[\![\exp(\rho_{\mathcal{E}}^\star + j\theta_{\mathcal{E}}^\star)]\!]$ and $\hat{Y}^f = Y^f[\![\exp(-\rho_{\mathcal{E}}^\star - j\theta_{\mathcal{E}}^\star)]\!]$. This equation can be further simplified to

$$y_{\mathcal{V}} - y_{\mathcal{V}}^d = Y_{\mathcal{V}\mathcal{E}}^+ \cosh(\delta\rho_{\mathcal{E}} + j\delta\theta_{\mathcal{E}}) + Y_{\mathcal{V}\mathcal{E}}^- \sinh(\delta\rho_{\mathcal{E}} + j\delta\theta_{\mathcal{E}}) \tag{24}$$

with the help of $Y^\pm = \hat{Y}^t \pm \hat{Y}^f$. Finally, using the $y - y^d = g + jb$ we obtain

$$\begin{bmatrix} g_{\mathcal{V}} \\ b_{\mathcal{V}} \end{bmatrix} = \begin{bmatrix} \mathrm{Re}(Y^+) & \mathrm{Re}(Y^-) & -\mathrm{Im}(Y^-) & -\mathrm{Im}(Y^+) \\ \mathrm{Im}(Y^+) & \mathrm{Im}(Y^-) & \mathrm{Re}(Y^-) & \mathrm{Re}(Y^+) \end{bmatrix} f(x) \tag{25}$$

where $f(x) = \begin{bmatrix} \cosh \delta\rho_{\mathcal{E}} \odot \cos \delta\theta_{\mathcal{E}} \\ \sinh \delta\rho_{\mathcal{E}} \odot \cos \delta\theta_{\mathcal{E}} \\ \cosh \delta\rho_{\mathcal{E}} \odot \sin \delta\theta_{\mathcal{E}} \\ \sinh \delta\rho_{\mathcal{E}} \odot \sin \delta\theta_{\mathcal{E}} \end{bmatrix}$.

The nonlinear vector $f(x)$ consists of element-wise products of the hyperbolic and trigonometric functions. To find the bounds $\delta_2 f^{\pm}$ which are required in the feasibility set construction (19), we apply nonlinear bounding introduced in Appendix B-A.

Like the traditional power flow equations, we use $x = (\theta_{\mathcal{G}}, \theta_{\mathcal{L}}, \rho_{\mathcal{L}})$ and consider only a subset of all the equations of the form $Ru = Mf(x)$:

$$\begin{bmatrix} g_{\mathcal{G}} \\ g_{\mathcal{L}} \\ b_{\mathcal{L}} \end{bmatrix} = \begin{bmatrix} \mathrm{Re}(Y^+_{\mathcal{GE}}) & \mathrm{Re}(Y^-_{\mathcal{GE}}) & -\mathrm{Im}(Y^-_{\mathcal{GE}}) & -\mathrm{Im}(Y^+_{\mathcal{GE}}) \\ \mathrm{Re}(Y^+_{\mathcal{LE}}) & \mathrm{Re}(Y^-_{\mathcal{LE}}) & -\mathrm{Im}(Y^-_{\mathcal{LE}}) & -\mathrm{Im}(Y^+_{\mathcal{LE}}) \\ \mathrm{Im}(Y^+_{\mathcal{LE}}) & \mathrm{Im}(Y^-_{\mathcal{LE}}) & \mathrm{Re}(Y^-_{\mathcal{LE}}) & \mathrm{Re}(Y^+_{\mathcal{LE}}) \end{bmatrix} f(x) \tag{26}$$

We define the parameter vector $\tilde{u}(V) = (p/V^2 - p^\star/(V^\star)^2, -q/V^2 + q^\star/(V^\star)^2)$ which consists of nodal admittance variations associated to the left hand side of (22). Further, let $V^- = V^\star - \delta V^-$. Assume that the nonlinear term $\phi(\tilde{x})$ is contained in the polytope $\mathcal{A}(\tau)$ where τ is defined in Lemma 2. Then Corollary 2 below is essential to characterize the admissible range of nodal power injections.

Corollary 2 (Admissible power injection estimation)**.** *For any $\tilde{u}$ such that $J_\star^{-1} R\, \tilde{u}(V^{\pm}) \in \mathcal{A}(\ell_x - \tau)$ there exists at least one admissible solution $\tilde{x} \in \mathcal{A}(\ell_x)$ of the equation (22). Further, given that $\tilde{u} \in \mathcal{U}(\ell_u)$, the allowed active power injection are as follows.*

$$\ell_p^- \le p \le \ell_p^+ \tag{27}$$

where $\ell_p^{\pm} = (V^-)^2 \left(\pm \ell_u^{\pm} + p^\star/(V^\star)^2\right)$. Similar bounds apply to the nodal reactive power.

Proof. Since $V^- \le V$ for all bus k, the condition $J_\star^{-1} R\tilde{u}(V^-) \in \mathcal{A}(\ell_x - \tau)$ implies that $J_\star^{-1} R\tilde{u}(V) \in \mathcal{A}(\ell_x - \tau)$. Following Theorem 3, this guarantees that (26) has a solution, so does (22). The range defined by (27) is a conservative estimation as we set $V = V^-$ and find the minimum and maximum values of the function $p = (V^-)^2(\tilde{u}(V^-) + p^\star/(V^\star)^2)$ with corresponding bounds on $\tilde{u}$. □

B. Thermal and reactive power constraints

Lemma 4 establishes a way to incorporate the feasibility constraints of the form $Tf(x) \le 0$ where $f(x)$ contains the element-wise products of the hyperbolic and trigonometric functions that appear in (26). Both thermal power and reactive power generation constraints can be presented in this form, and below we will show the corresponding coefficient matrix T.

a) Thermal power constraint: by following the sequence from (21) to (25), we can derive an equivalent admittance based expression for the power transfers. The power transfers "to" and "from" for each line are very similar, thus we only present the "from" transmission.

The current on line $e = (k, j)$ can be represented as:

$$i_e^f = Y_e^f v_{\mathrm{to}(e)} + Y_e^t v_{\mathrm{from}(e)}. \tag{28}$$

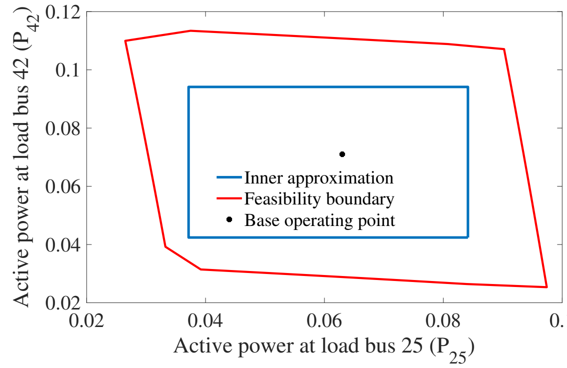

Fig. 3. Feasibility set of an OPF for IEEE 57-bus system

where $\mathrm{from}(e) = k$ and $\mathrm{to}(e) = j$. Let $y_e^f = \overline{(s_e^f)}/V_k^2$ and $y_e^f - Y_e^t = g_e^f + \mathbf{j} b_e^f$. By repeating the admittance base derivation, we ultimately yield the following expression:

$$\begin{bmatrix} g_{\mathcal{E}}^f \\ b_{\mathcal{E}}^f \end{bmatrix} = \begin{bmatrix} \mathrm{Re}(Y^+_{\mathcal{E}}) & \mathrm{Re}(Y^-_{\mathcal{E}}) & -\mathrm{Im}(Y^-_{\mathcal{E}}) & -\mathrm{Im}(Y^+_{\mathcal{E}}) \\ \mathrm{Im}(Y^+_{\mathcal{E}}) & \mathrm{Im}(Y^-_{\mathcal{E}}) & \mathrm{Re}(Y^-_{\mathcal{E}}) & \mathrm{Re}(Y^+_{\mathcal{E}}) \end{bmatrix} f(x) \tag{29}$$

where $Y^{\pm}_{\mathcal{E}} = \pm \Delta_{\mathcal{VE}} \hat{Y}^f_{\mathcal{VE}}$, and the entry $\Delta_{k,e}$ becomes 1 only when $k = \mathrm{from}(e)$ and is 0 otherwise. Then the auxiliary matrix T is easily obtained from (29).

Concerning the thresholds on the apparent power transfer, we propose to enforce intermediate constraints on the active and reactive power transfers, i.e., $\ell^-_{p,e} \le p_e \le \ell^+_{p,e}$ and $\ell^-_{q,e} \le q_e \le \ell^+_{q,e}$. These intermediate constraints can be easily expressed in the form of $h(x) \le 0$ which later can be incorporated in the framework (19) with the form of the last set of constraints. Then, the limit on the apparent power can be guaranteed by an extra condition $(\ell^{\pm}_{p,e})^2 + (\ell^{\pm}_{q,e})^2 \le (s_e^{max})^2$.

b) Reactive power generation constraint: Like the load power and active power generation presented in (26), the reactive generation can be easily represented using an admittance form. Thus, the associated matrix T is simply the following:

$$-\begin{bmatrix} \mathrm{Im}(Y^+_{\mathcal{GE}}) & \mathrm{Im}(Y^-_{\mathcal{GE}}) & \mathrm{Re}(Y^-_{\mathcal{GE}}) & \mathrm{Re}(Y^+_{\mathcal{GE}}) \end{bmatrix} \tag{30}$$

In like manner as the thermal limits, we impose conditions on reactive power generation level by introducing intermediate constraints $\ell_q^- \le q \le \ell_q^+$. Then the reactive limits are enforced simply as $q^{min} \le \ell_q^- \le \ell_q^+ \le q^{max}$.

V. Simulations

For our algorithm validation and simulations, we relied on transmission test cases included in the MATPOWER package and constructed the inner approximations for all the cases up to 1354 buses. We also compared our constructed regions to the cross-sections of the actual feasibility sets to assess the conservativeness of the approach. The problem specifications and the details of the construction are presented below.

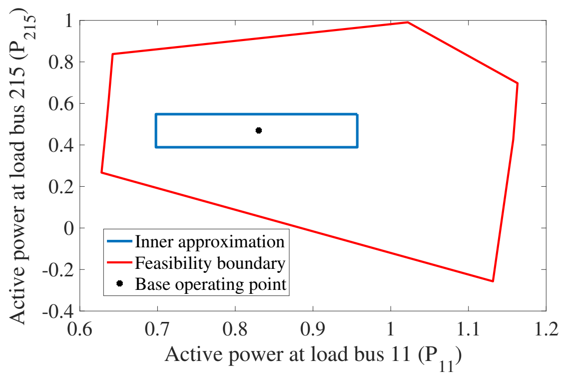

Fig. 4. Feasibility set of an OPF for IEEE 300-bus system

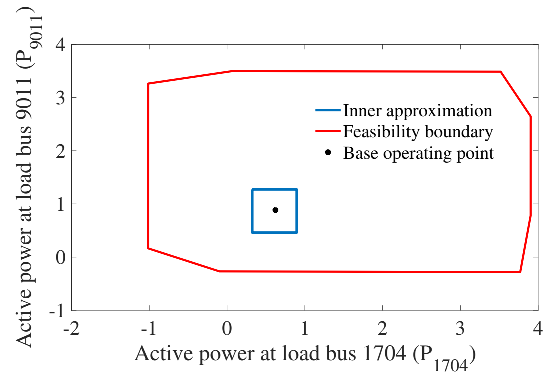

Fig. 5. Feasibility set of an OPF for 1354-bus medium part of European system

A. OPF problem setup

A typical OPF problem, which is previously introduced in section I, considers both power flow equality constraints (1), and operational constraints (2-6) including nodal voltage and angle limits, power generation limits, and thermal limits. While the voltage regulation standards require a voltage deviation of $\pm 5\%$ from the nominal voltage level of $1 p.u.$, some base cases available in the MATPOWER package may be not compliant. To deal with this issue, we constrain the voltage to stay within 1% around the base voltage level $x^\star$.

For the power generation limits, we adopt the data from the available MATPOWER test cases. The line thermal limits, however, are not provided, so for the sake of simplicity, we assume that the maximum power transfer level is double the corresponding value of the base operating condition, i.e., $s_e^{max} = 2|s_e^\star|$. The reactive power generation and thermal limits are considered for all test cases with less than 300 buses. However, we exclude them while simulating 300- and 1354-bus systems as the actual feasibility margins become extremely small for the default base operating points.

B. Feasibility region construction

Upon setting up the OPF, we can solve problem (19) to identify the "optimal" feasibility sets. In the following simulations, we extensively construct the optimal sets which maximize the uniformly boxed loading variations or the robustness certificate discussed in section III-A2. For simplicity, we focus on the loading pattern $\tilde{u}$ with only two load injection variations, and we duly visualize the estimated feasibility sets in the corresponding 2D plane as shown in Figure 3 to Figure 5.

As discussed in section III, it is more efficient for large-scale test cases to start with the LP version of the construction (19) instead with the nonlinear one. Although the LP optimal solution later can be further improved by using nonlinear optimization solvers, in this work, we apply directly the LP solution to construct all the approximated feasibility sets as the results are sufficiently large.

To evaluate the inner approximation technique, we compare the estimations with the real feasible sets. Unlike the estimated feasibility boundary which can be characterized entirely at one time, the actual boundary relies on a numerical and point-wise construction scheme. More specifically, we use Continuation Power Flow [22] to trace the critical points along multiple loading directions, then the actual boundary is created by connecting all such critical points.

In most cases, as shown in Figures 3 to 5, the approximated sets cover a large fraction of the true feasible domains. As the considered test systems may be very different concerning network properties like topology and line parameters, the proposed technique is proven to be stable and effectual to a wide variety of transmission systems. It is important to note that some large-scale cases like the 300-bus system, which has abnormally high reactive power compensation, or considerably huge systems like the European network can easily induce extremely conservative estimations due to improper bounding nonlinearities. Specifically, the nonlinear terms relating to the angle separation can grow quickly, this subsequently suppresses the allowed variation of the power injection inputs. The admittance base representation presented in section IV-A is a non-trivial form which bounds the angle separation while ensuring the convexity of the polytope $\mathcal{A}$, thus playing an important role in guaranteeing the effectiveness of the proposed technique.

Another interesting observation is that, along some loading directions, the gap between the two boundaries is almost zero. It may be of interest to understand under which condition one can achieve such a coalescence; however, apart from that observed in the simulations, in the scope of this paper, we do not provide any further rigorous analysis.

VI. Conclusion

To conclude, in this work we developed a novel framework for constructing inner approximations of the OPF feasible set that does not rely on any extra modeling assumptions and is applicable for typical transmission systems. The framework is based on Brouwer fixed point theorem, which is applied to polytopic regions in voltage-angle space. In comparison to other studies of the same problem, our framework is not entirely analytic and instead relies on nonlinear optimization procedures to find the largest feasible sets that possess the self-mapping property.

The optimization framework can naturally be applied to a number of most common settings, ranging from the classical loadability problem to robustness analysis, and chance constraint certification. Such a nonlinear optimization problem is non-convex and likely NP-hard; however, any feasible solution even not globally optimal one is a valid certificate. Furthermore, the complexity of the problem scales linearly in the system size, and valid certificates can be constructed with computational effort comparable to solving the original OPF problem. Simulation results show that the proposed technique is scalable and can provide sufficiently large estimations.

The estimation heavily depends on how tightly the nonlinear map (13) can be bounded, and the results can be improved by using more adaptive bounds. Particularly, to approximate the nonlinear function, we can use more faced polytopes instead of simple hyper-rectangles like the ones plotted in Figure 2. Moreover, as some nonlinear functions appearing in the fixed point map will not contribute significantly to the conservativeness of the inner approximation, there is no need to use adaptive bounds for all, but the most effectual individuals.

The framework can be extended to security-constrained OPF concerning contingency analysis, typically $N-1$ line contingency. If we can bound the effect of one line failure on matrix M in (7) and consequently on the correction term $\phi(\tilde{x})$, the nonlinear fixed point map can be bounded accordingly. Then we can apply the self-mapping condition to ensure the existence of a solution subject to one line tripping condition.

REFERENCES

[1] M. B. Cain, R. P. Oneill, and A. Castillo, “History of optimal power flow and formulations,” *Federal Energy Regulatory Commission*, pp. 1–36, 2012.

[2] R. A. Jabr, “Radial distribution load flow using conic programming,” *IEEE transactions on power systems*, vol. 21, no. 3, pp. 1458–1459, 2006.

[3] J. Lavaei and S. H. Low, “Zero duality gap in optimal power flow problem,” *IEEE Transactions on Power Systems*, vol. 27, no. 1, pp. 92–107, Feb 2012.

[4] C. Coffrin, H. L. Hijazi, and P. Van Hentenryck, “The qc relaxation: A theoretical and computational study on optimal power flow,” *IEEE Transactions on Power Systems*, vol. 31, no. 4, pp. 3008–3018, 2016.

[5] B. Cui and X. A. Sun, “A new voltage stability-constrained optimal power flow model: Sufficient condition, socp representation, and relaxation,” *arXiv preprint arXiv:1705.10372*, 2017.

[6] D. K. Molzahn, V. Dawar, B. C. Lesieutre, and C. L. DeMarco, “Sufficient conditions for power flow insolvability considering reactive power limited generators with applications to voltage stability margins,” in *IREP Symposium*. IEEE, 2013, pp. 1–11.

[7] E. Hnyilicza, S. Lee, and F. Schweppe, “Steady-state security regions: The set theoretic approach,” in *Proc. 1975 PICA Conf.*, 1975, pp. 347–355.

[8] F. F. Wu and S. Kumagai, “Steady-state security regions of power systems,” *Circuits and Systems, IEEE Transactions on*, vol. 29, no. 11, pp. 703–711, 1982.

[9] V. Vasin, “Regions of power system operating point existence and their analytic estimates,” *internal report of Energoset’proekt (in Russian)*, 1985.

[10] F. Byc, B. Kobets, N. Nesterenko, and E. Zel’manov, “An approach for decentralized evaluation of regimes in power systems,” in *Fifth international conference on present day problems of power system automation and control, Gliwice*, 1989, pp. 297–301.

[11] S. Bolognani and S. Zampieri, “On the existence and linear approximation of the power flow solution in power distribution networks,” *IEEE Transactions on Power Systems*, vol. 31, no. 1, pp. 163–172, 2016.

[12] S. Yu, H. D. Nguyen, and K. S. Turitsyn, “Simple certificate of solvability of power flow equations for distribution systems,” in *2015 IEEE Power Energy Society General Meeting*, July 2015, pp. 1–5.

[13] C. Wang, A. Bernstein, J.-Y. Le Boudec, and M. Paolone, “Existence and uniqueness of load-flow solutions in three-phase distribution networks,” *IEEE Transactions on Power Systems*, 2016.

[14] H. D. Nguyen, K. Dvijotham, S. Yu, and K. Turitsyn, “A framework for robust steady-state voltage stability of distribution systems,” *arXiv preprint arXiv:1705.05774*, 2017.

[15] J. W. Simpson-Porco, F. Dörfler, and F. Bullo, “Voltage collapse in complex power grids,” *Nature communications*, vol. 7, 2016.

[16] J. W. Simpson-Porco, “A theory of solvability for lossless power flow equations–part i: Fixed-point power flow,” *IEEE Transactions on Control of Network Systems*, 2017.

[17] J. W. Simpson-Porco, “A theory of solvability for lossless power flow equations–part ii: Conditions for radial networks,” *IEEE Transactions on Control of Network Systems*, vol. PP, no. 99, pp. 1–1, 2017.

[18] K. Dvijotham and K. Turitsyn, “Construction of power flow feasibility sets,” *ArXiv e-prints*, Jun. 2015.

[19] K. Dvijotham, H. Nguyen, and K. Turitsyn, “Solvability regions of affinely parameterized quadratic equations,” *IEEE Control Systems Letters*, vol. 2, no. 1, pp. 25–30, Jan 2018.

[20] H. D. Chiang and C. Y. Jiang, “Feasible region of optimal power flow: Characterization and applications,” *IEEE Transactions on Power Systems*, vol. PP, no. 99, pp. 1–1, 2017.

[21] E. H. Spanier, *Algebraic topology*. Springer Science & Business Media, 1994, vol. 55, no. 1.

[22] V. Ajjarapu and C. Christy, “The continuation power flow: a tool for steady state voltage stability analysis,” *IEEE transactions on Power Systems*, vol. 7, no. 1, pp. 416–423, 1992.

APPENDIX A
OPTIMAL CONSTRUCTION VALIDATION

To validate the construction of optimal inner approximation (19), which is the main result introduced in section III, we will show that the imposed constraints guarantee the existence of a feasible solution. In particular, as we show below, such constraints are sufficient conditions for solvability and feasibility.

A. Solvability condition

The goal of this section is to verify that the following condition, which is the first set of constraints in (19), is sufficient for the solvability of the equality constraints (7)

$$\ell_x^{\pm} \geq B^+\ell_u^{\pm} + B^-\ell_u^{\mp} + C^+\delta_2 f^{\pm}(\ell_x) + C^-\delta_2 f^{\mp}(\ell_x). \quad (31)$$

Specifically, we reply on Corollary 1 and later Corollary 3 to show that the above constraint verifies self-mapping condition, thus defining a solvability subset $\mathcal{U}(\ell_u)$. The following Lemma 2 and Theorem 3 helps prepare Corollary 3.

Lemma 2. *Given the nonlinear system described by the equation* (14) *the admissibility and nonlinear bound polytope families* $\mathcal{A}(\ell_x)$ *and* $\mathcal{N}(\ell_x)$*, if* $\tilde{x} \in \mathcal{A}(\ell_x)$ *then the nonlinear correction term* $\phi(\tilde{x})$ *is contained in the polytope* $\mathcal{A}(\tau(\ell_x))$*, i.e.* $\phi(\tilde{x}) \in \mathcal{A}(\tau(\ell_x))$ *with* $\tau(\ell_x) = [-\tau^-(\ell_x), \tau^+(\ell_x)] \in \mathbb{R}_+^{k\times 2}$ *given by*

$$\tau^{\pm}(\ell_x) = C^+\delta_2 f^{\pm}(\ell_x) + C^-\delta_2 f^{\mp}(\ell_x) \quad (32)$$

where $C^+ - C^- = -AJ_\star^{-1}M$ *and* $C_{ij}^{\pm} \geq 0$.

Proof. This bound generalizes the definition of a matrix $\infty-$ norm and follows directly from bounding individual contributions to $A\phi(\tilde{x})$ with the help of the non-negativity of $\delta_2 f^{\pm}$. $\square$

Remark: It can be observed that the map $\tau(\ell_x) : \mathbb{R}_+^{k\times 2} \to \mathbb{R}_+^{k\times 2}$ is monotone because increasing the region of variable variations can only increase the region of possible nonlinear corrections.

Theorem 3. *Given all the definitions above, assume that there exists a matrix ℓ_x, such that the matrix $\tau(\ell_x)$ as defined in the Lemma 2 satisfies $\tau^{\pm}(\ell_x) \leq \ell_x^{\pm}$. Then, for any $\tilde{u}$ such that $J_\star^{-1} R\tilde{u} \in \mathcal{A}(\ell_x - \tau(\ell_x))$ there exists at least one admissible solution $\tilde{x} \in \mathcal{A}(\ell_x)$ of the equation* (14).

Proof. The right hand side of (14) is contained in the polytope $\mathcal{A}(\ell_x)$, therefore the map $F(\tilde{x}) = J_\star^{-1}\tilde{s} + \phi(\tilde{x})$ maps the compact convex set $\mathcal{A}(\ell_x)$ onto itself. Thus, according to Brouwer's theorem, there exists a fixed point $\tilde{x} = F(\tilde{x})$ inside $\mathcal{A}(\ell_x)$. □

Corollary 3. *The admissible solution $\tilde{x}^\star \in \mathcal{A}(\ell_x)$ is guaranteed to exists for every element $\tilde{u}$ inside a box-shaped uncertainty set $\mathcal{U}(\ell_u)$ whenever the condition*

$$\ell_x^{\pm} \geq \sigma^{\pm}(\ell_u) + \tau^{\pm}(\ell_x) \tag{33}$$

$$\sigma^{\pm}(\ell_u) = B^+\ell_u^{\pm} + B^-\ell_u^{\mp} \tag{34}$$

is satisfied with $B^+ - B^- = AJ_\star^{-1}R$ and $B_{ij}^{\pm} \geq 0$.

Proof. Whenever $\tilde{u} \in \mathcal{U}(\ell_u)$, one has $-\sigma^-(\tilde{u}) \leq AJ_\star^{-1}R\tilde{u} \leq \sigma^+(\tilde{u})$, hence the inputs satisfy the conditions of Theorem 3. □

Substituting (34) and (32) into the self-mapping condition (33), yields the sufficient condition for solvability (31).

B. Feasibility conditions

As the self-mapping condition (33) verifies the existence of a solution, we complete validating the central optimization problem (19) by proving the feasibility. In particular, the voltage level and angle separation limits presented in (8) can be easily imposed with the element-wise upper bounds on the fixed point variables, i.e., $x^{min} \leq x^\star - \ell_x^- \leq x^\star + \ell_x^+ \leq x^{max}$. These constraints can be rewritten in a compact form as $\ell_x \leq \ell_x^{max}$ in (19).

Next, we consider the remaining feasibility constraints $h(x) \leq 0$, which is introduced in (9). The following theorem, which facilitates the incorporating of feasibility conditions, contribute to the last constraints of the construction (19).

Lemma 4. *(Feasibility conditions) The nonlinear feasibility constraints $h(x) \leq 0$ will be satisfied if the following condition holds.*

$$D^+\ell_u^+ + D^-\ell_u^- + E^+\delta_2 f^+(\ell_x) + E^-\delta_2 f^-(\ell_x) + h_\star \leq 0 \tag{35}$$

where $D = TLJ_\star^{-1}R$, $E = T - TLJ_\star^{-1}M$, and $L = \frac{\partial f}{\partial x}|_{x_\star}$.

The theorem can be proved as the following. Using the definition of the residual operator $\delta_2 f$, yields the below expansion.

$$\begin{aligned} h(x) &= h_\star + TL\tilde{x} + T\delta_2 f \\ &= h_\star + TLJ_\star^{-1}R\delta u + (T - TLJ_\star^{-1}M)\delta_2 f. \end{aligned} \tag{36}$$

The second equality can be derived with the help of the fixed point equation (14). Then the left hand side of (35), which is represented using ∞ norm type bound (32) and (34), essentially constitutes an upper bound of the function $h(x)$ in constraint (9). Thus, the condition (35) is sufficient for (9).

Appendix B
Nonlinear bounding and LP relaxation

A. Nonlinear bounding

The bounds on the individual nonlinear terms of $f(x)$ can be expressed as:

$$\delta_{1,2}^+\{\cos\delta\theta_e\} = 0 \tag{37a}$$
$$\delta_{1,2}^-\{\cos\delta\theta_e\} = \max\{1 - \cos\delta\theta_e^+, 1 - \cos\delta\theta_e^-\} \tag{37b}$$
$$\delta^{\pm}\{\sin\delta\theta_e\} = \sin\delta\theta_e^{\pm} \tag{37c}$$
$$\delta_2^{\pm}\{\sin\delta\theta_e\} = \delta\theta_e^{\mp} - \sin\delta\theta_e^{\mp} \tag{37d}$$
$$\delta_{1,2}^-\{\cosh\delta\rho_e\} = 0 \tag{37e}$$
$$\delta_{1,2}^+\{\cosh\delta\rho_e\} = \max\{\cosh\delta\rho_e^+, \cosh\delta\rho_e^-\} - 1 \tag{37f}$$
$$\delta^{\pm}\{\sinh\delta\rho_e\} = \sinh\delta\rho_e^{\pm} \tag{37g}$$
$$\delta_2^{\pm}\{\sinh\delta\rho_e\} = \sinh\delta\rho_e^{\pm} - \delta\rho_e^{\pm} \tag{37h}$$

Then we will apply the following corollary and theorem to derive the residual operator $\partial_2 f$ and the bounds on products of nonlinearities.

Corollary 4. *For the element-wise product of two vector functions $f(x) \odot h(x)$ one has*

$$\delta_2\{f \odot g\} = \delta f \odot \delta g + \delta_2 f \odot g^\star + f^\star \odot \delta_2 g \tag{38}$$

This can be proved directly following the definitions of the residual operators.

Lemma 5. *Bounds on the products can be characterized in the following way:*

$$\begin{aligned} \delta_2^{\pm}\{f \odot g\} = \max\{\delta f^+ \odot \delta g^{\pm}, \delta f^- \odot \delta g^{\mp}\} \\ + f^\star \odot \delta_2 g^{\pm} + \delta_2 f^{\pm} \odot g^\star \end{aligned} \tag{39}$$

which is shorthand for two estimations with corresponding superscript $+$ and $-$.

B. Extension using LP relaxation

Here we derive the linear bounds for the nonlinear function $\phi(\tilde{x})$ which will form the LP version of problem (19). We constraint all the angles within $\pm\theta^U$, and all logarithmic voltages ρ within $\pm\rho^U$. Let define $\delta\theta_e^m = \max\{\delta\theta_e^{\pm}\}$ and $\delta\rho_e^m = \max\{\delta\rho_e^{\pm}\}$ where $\pm\theta \leq \theta^{\pm} \leq \theta^U \leq \pi/2$, $\theta^m = \max\{\theta^{\pm}\}$, and $0 \leq \rho \leq \rho^U \leq 1$. The relaxation is as follows.

$$1 - \cos(\theta) \leq (1 - \cos(\theta^U))\frac{\theta^m}{\theta^U} \tag{40}$$

$$\sin(x) \leq (\theta^U - \sin(\theta^U))\frac{\theta}{\theta^U} \tag{41}$$

$$\cosh(\rho) - 1 \leq (\cosh(\rho^U) - 1)\frac{\rho}{\rho^U} \tag{42}$$

$$\sinh(\rho) \leq \sinh(\rho^U)\frac{\rho}{\rho^U} \tag{43}$$

For product terms, we need McCormick envelopes: $xy \leq x^U y + xy^L - x^U y^L$ and $xy \leq xy^U + x^L y - x^L y^U$.